Nano-Optomechanical Resonators Based Graphene/Au Membrane for Current Sensing

Shen Liu, Peijing Chen, Junxian Luo, Yanping Chen, Bonan Liu, Hang Xiao, Wenqi Yan, Wei Ding, Zhiyong Bai, Jun He, and Yiping Wang, *Senior Member, IEEE*

***Abstract*—The monitoring of electric current is essential to ensuring the reliable operation of power systems and electronic equipment. The present study demonstrates an optomechanical cavity-based resonator suitable for current sensing. The proposed device consists of a suspended graphene/Au membrane supported by a ceramic ferrule with a bore diameter of approximately 125 μm and incorporates optical actuation and detection processes. The present sensor exhibits high current sensitivities of approximately 7.91 and 18.04 Hz/mA^2 when monitoring the resonant frequency at first and second-order vibrational modes. This optomechanical current sensor operates for the first time in the 100 mA range, an advance of more than two orders of magnitude on the sole previously reported cavity optomechanical current sensor. Moreover, the current sensor shows a short response time of ∼2 ms and provides the additional advantages of low power consumption and a compact structure. This device is expected to have applications in high-precision current and magnetic field sensing.**

***Index Terms*—Current sensor, optical fiber sensor, optomechanical resonator.**

I. Introduction

MICRO- and nanomechanical resonators that vibrate at high frequencies provide the advantages of small sizes and ultralow masses. These resonators have also exhibited ultra-high sensitivity during the measurement of force [1], [2] mass [3], [4], and [5], pressure [6] and thermal radiation [7], [8], during which mechanical vibrations are converted into a measurable electrical or optical output signal. The electrostatic forces generated by gate voltages have been widely used to actuate these micro/nanomechanical resonators, but this mechanism has various associated deficits, including nonlinear outputs, the potential for short-circuiting and the requirement to apply high driving voltages [9]. Optical actuation has been proposed as an effective means of addressing these issues based on the direct coupling of modulated light power with the resonator. Various micro- and nanomechanical resonators for sensing based on optical actuation and readout systems have been developed, including optomechanical magnetometers [10], [11], single molecule detection [12], cavity optomechanical ultrasound sensors [13]and all-optical photothermal sensors [14]. Furthermore, opto-mechanical coupling is realized by Optical actuation in the micro- and nanomechanical resonators and is widely used in nonlinear optics [15], optomechanically induced transparency [16], optical storage [17], [18], and optomechanical cooling [19].

Compared with commercial current sensors using electronic sensing components, fiber optic current sensors have attracted more attention because these sensors provide the intrinsic advantages of avoiding electromagnetic interference, minimal security risks, and remote measurement capabilities. However, the majority of present-day fiber optic sensors are based on the Faraday effect [20], [21], and [22] and tend to be quite bulky as a consequence of the small Verdet constants of optical fibers [23]. In addition, this type of sensor is associated with issues related to accuracy because of the linear birefringence inherent in optical fibers [24]. Current can also be measured by combining magnetostrictive materials with fiber gratings and measuring the drift of the grating wavelength [25], [26], and [27]. This is an indirect measurement method that relies on the conversion of current to magnetic field. Another approach that appears viable is to take advantage of thermal effects to realize current sensing. Typically, these sensors used graphene membrane as a sensor element for current sensing [28], [29]. However, the current detecting range of these current sensors is restricted due to thin graphene cannot sustain high current.

The present work demonstrates an optical fiber current sensor based on an optomechanical cavity concept. This optical mechanical current sensor uses graphene/Au composite membrane with higher current carrying capacity as the current sensing element. It operates in the 100 mA range, which is two orders of magnitude greater than the ranges of previously reported optomechanical current sensors [29]. This device was fabricated by transferring multilayer graphene to the end facet of a ceramic

Manuscript received 24 May 2022; revised 3 August 2022; accepted 7 August 2022. Date of publication 11 August 2022; date of current version 4 November 2022. This work was supported in part by the National Natural Science Foundation of China (NSFC) under Grants 62175165, 61905165, 61875134, and 62005169, in part by Guangdong Basic and Applied Basic Research Foundation under Grant 2021A1515011834, in part by the Foundation for Distinguished Young Talents in Higher Education of Guangdong under Grant 2018KQNCX219, in part by Shenzhen Science and Technology Program under Grants RCBS20200714114922296, JCYJ20210324120403009, and JCYJ20180507182058432, and in part by the Postgraduate Innovation Development Fund Project of Shenzhen University under Grant 315-0000470804. *(Corresponding author: Zhiyong Bai.)*

The authors are with the Shenzhen Key Laboratory of Photonic Devices and Sensing Systems for Internet of Things, College of Physics and Optoelectronic Engineering, Shenzhen University, Shenzhen 518060, China, and also with the Guangdong and Hong Kong Joint Research Centre for Optical Fibre Sensors, Shenzhen University, Shenzhen 518060, China (e-mail: shenliu@szu.edu.cn; 2070456073@email.szu.edu.cn; 1810285012@email.szu.edu.cn; chenyanping2019@email.szu.edu.cn; ssamliu@163.com; 2060453045@email.szu.edu.cn; yanwenqi2020@email.szu.edu.cn; 2110456062@email.szu.edu.cn; baizhiyong@szu.edu.cn; hejun07@szu.edu.cn; ypwang@szu.edu.cn).

Color versions of one or more figures in this article are available at https://doi.org/10.1109/JLT.2022.3198116.

Digital Object Identifier 10.1109/JLT.2022.3198116

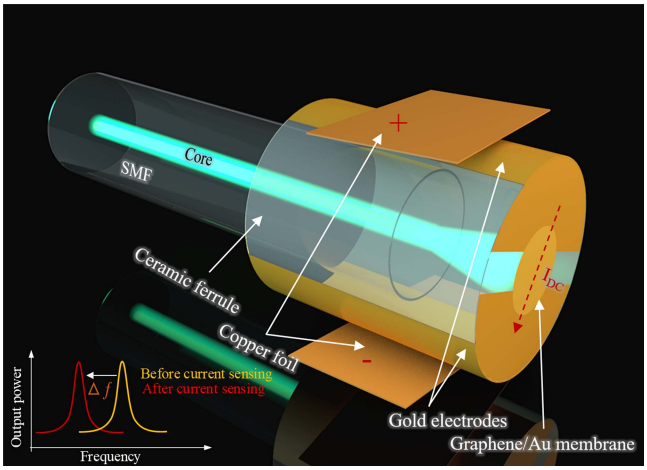

Fig. 1. Diagram of the present fiber optic current sensor based on a graphene/Au membrane.

ferrule followed by applying an Au layer with a thickness of approximately 75 nm to form a Fabry-Perot (F-P) cavity between the graphene/Au membrane and the end face of the optical fiber. Two electrodes were subsequently etched onto the end face of the ceramic ferrule using a femtosecond laser. This resonator was actuated by a modulated pump laser and the resulting signal was detected using a continuous wave laser. As a result of Joule heating, any additional current flowing through the membrane increased its temperature, resulting in a shift in its resonant frequency. This sensor demonstrated high current sensitivities of approximately 7.91 and 18.04 Hz/mA^2 at resonance frequencies of 221.4 and 490.5 kHz, respectively. These sensitivities could potentially be increased by improving the quality factor, Q, of the sensor based on vacuum encapsulation of the device. Moreover, a design strategy using an optomechanical cavity evidently provides excellent recoverability. The present work demonstrates that the integration of graphene/Au nanomaterials and fiber optic sensing technology can provide a novel, compact and sensitive sensor having a wide working range.

II. Principles

Fig. 1 provides a diagram of the suspended graphene/Au membrane-based current sensor fabricated in the present work. This device comprised a standard single mode fiber (SMF, Corning Inc., SMF-28), a ceramic ferrule and a graphene/Au membrane. Where, a pair of gold electrodes are employed to apply the current into the graphene/Au composite membrane. The electrode is clamped by two copper foils connecting an external current source, and the current could be coupled into the graphene/Au membrane to realize sensing application. In this sensor, two partially reflective mirrors, i.e., the graphene/Au membrane and the fiber end facet, form an optomechanical cavity resonator, of which the resonant frequency is modified by joule heating induced from a small current change. Here, the all-optical excitation and readout method is employed by the current sensor based on the optomechanical cavity resonator. The mechanical resonance of a thin circular membrane can be calculated as [30]

$$f_0 = \frac{2.404}{\pi d}\sqrt{\frac{\gamma_{300k}}{\rho t}} \tag{1}$$

where d is the diameter of the membrane, $\gamma_{300\mathrm{K}}$ is the initial built-in tension at 300 K (in unit of N/m), ρ is the density of the membrane and t is the thickness of the membrane. Upon applying a current, the temperature of the membrane increases and the resulting change in tension affects the resonance frequency based on the relationship [31], [32]

$$f_0 = \frac{2.404}{\pi d}\sqrt{\frac{\gamma_{300k} + \gamma_T}{\rho_{eff} t_{eff}}} \tag{2}$$

where γ_{T} is the additional tension induced by the temperature change. Note that the present membrane had a double layer structure comprising layers of graphene and Au and so this equation uses both an effective density, ρ_{eff}, and effective thickness, t_{eff}, calculated as [33]

$$t_{eff} = t_g + t_{Au} \tag{3}$$

And

$$\rho_{eff} = \frac{\rho_g t_g + \rho_{Au} t_{Au}}{t_g + t_{Au}} \tag{4}$$

where t_{g} and t_{Au} are the graphene and Au thicknesses, respectively, and ρ_g and ρ_{Au} are the graphene density and the Au density, respectively.

III. Sensor Fabrication and Spectral Analysis

The sensor was fabricated by first transferring six to eight layers of multilayer graphene (Six Carbon Technology, Shenzhen, China) to the end face of a ceramic ferrule having a bore diameter of 125 μm using a wet transfer method. The graphene plays important roles. Firstly, it is a support for the deposition of Au on the hole of ferrule while magnetron sputtering is employed. The graphene has exceptional mechanical characteristics, such as Young's modulus of up to 1 TPa and inherent strength of up to 130 GPa, which makes it very suitable for supporting Au membrane [34]. Secondly, by using graphene/Au composite membrane as the current sensing element, the current carrying capacity of the composite membrane can be improved to withstand a larger current measurement range. In addition, graphene can firmly adhere to the end face of the ceramic ferrule through van der Waals force, which increases the stability of the graphene/Au composite membrane. The details of the wet transfer technique have been previously described in the literature [35]. In preparation for depositing the Au membrane, the ceramic ferrule was fixed inside the sputtering chamber with the end facet facing the Au target. During sputtering, a rotating fixture was used to ensure a uniform coating and the Au thickness was controlled by adjusting the sputtering time. A portion of the Au membrane on either side of the ceramic ferrule was subsequently removed using two pieces of lapping films, leaving two parallel gap structures. The Au membrane on the end surface of the ceramic ferrule was then etched with a fs laser ($\lambda = 514$ nm) pulsing at a rate of 200.488 kHz. The laser beam

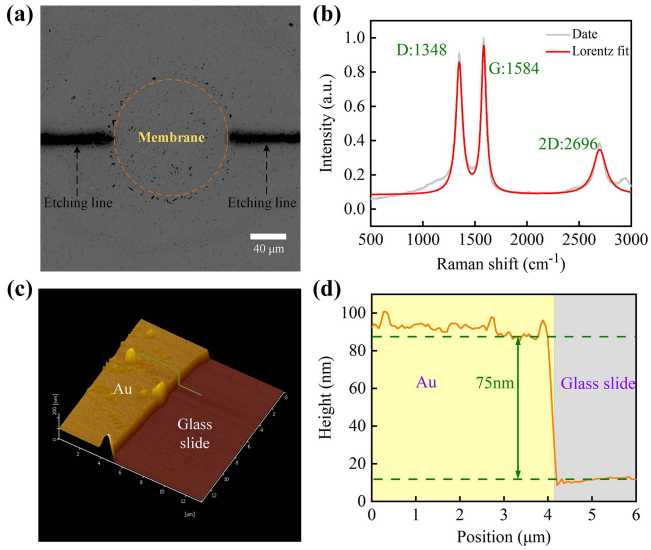

Fig. 2. (a) An SEM image of the ceramic ferrule end facet with the membrane in place. (b) Raman spectrum of graphene acquired using a 532 nm laser. (c) Atomic force microscopy image of the Au-coated glass slide. (d) The height profiles of the Au membrane.

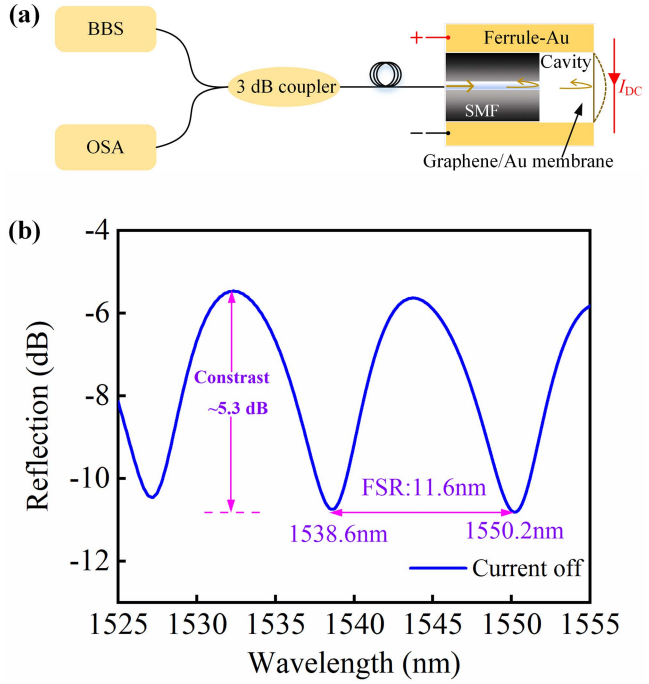

Fig. 3. (a) The optical measurement set-up. (b) A typical reflectance spectrum obtained from the FP interferometer made with a graphene/Au membrane. Legend: BBS = broadband light source, OSA = optical spectrum analyzer.

was focused onto the ceramic ferrule end facet through a 20× objective lens with a numerical aperture of 0.29 and a working distance of 30 mm to form a small channel corresponding to the lateral gaps. In this manner, a ceramic ferrule with two separated electrodes was obtained such that the current only flowed through the graphene/Au membrane. The graphene and Au membranes are combined to form a composite membrane as a current sensing element. The current flows in the composite membrane at the same time, where it is regarded as an entirety sensing element due to the graphene and Au have the same order of magnitude resistivity (about 10^{-6} Ω· cm) [36], [37]. Here, the resistance of graphene/Au composite membrane is measured to be about 20 Ω. Finally, an SMF having a precisely cut end facet was inserted into the other end of the ceramic ferrule using a high-precision displacement platform, such that the end face of the SMF and the graphene/Au membrane formed an FP cavity interferometer. The distance between the end face of the SMF and the graphene/Au membrane equaled the initial cavity length, L, of the FP cavity and this value could be adjusted by tuning the displacement platform and subsequently calculated by reflectance spectroscopy. Furthermore, the tail fiber was fixed with glue.

Fig. 2(a) shows a scanning electron microscopy (SEM) image of the end face of the ceramic ferrule covered with the graphene/Au membrane. Fig. 2(b) presents the Raman spectrum of the transferred graphene membrane on the ceramic ferrule end facet together with a Lorentz fit to the data. This spectrum exhibits three characteristic graphene peaks at 1348, 1584 and 2696 cm^{-1}. The energy difference between the D and G peaks corresponds to that expected for six to eight layers of graphene [38]. During the sputtering process, a glass slide was placed at the same height as the ceramic ferrule's end face to allow the thickness of the Au membrane to be determined. The thickness of the Au layer deposited on this slide was measured using atomic force microscopy as shown in Fig. 2(c). Fig. 2(d) presents the height profiles along the green line in Fig. 2(c), from which the thickness was estimated to be approximately 75 nm.

Fig. 3(a) shows a diagram of a typical measurement set-up employed to obtain the reflectance spectrum of the FP interferometer. This apparatus comprised a broadband light source, a 3 dB fiber coupler and an optical spectrum analyzer. Fig. 3(b) presents a typical spectrum acquired from a resonator over the wavelength range of 1525 to 1555 nm. The free spectrum range (FSR) of the resonator was approximately 11.6 nm, corresponding to wavelengths of 1538.6 and 1550.2 nm. Based on these data, the length of the FP cavity was calculated using the formula $L = \lambda_1\lambda_2/2n_{\text{air}}(\lambda_1\text{-}\lambda_2)$, where n_{air} is the refractive index of air and λ_1 and λ_2 are the wavelengths of adjacent valleys in the spectrum. In this manner, the length of the FP cavity was found to be approximately 102.8 μm. The contrast of FP reflection spectrum depends on the reflectivity of fiber end face (4%) [39] and graphene/Au membrane, where the thickness of the Au membrane is about 75 nm with more than 90% optical reflectivity. Therefore, the interference fringe contrast is about 5.3 dB, which is attributed to great difference in reflectivity between Au membrane and SMF end face. This interference fringe contrast could potentially be improved in two ways. One approach would be to reduce the intensity of light reflected from the graphene/Au membrane by increasing the cavity length and the other would involve reducing the thickness of the Au membrane.

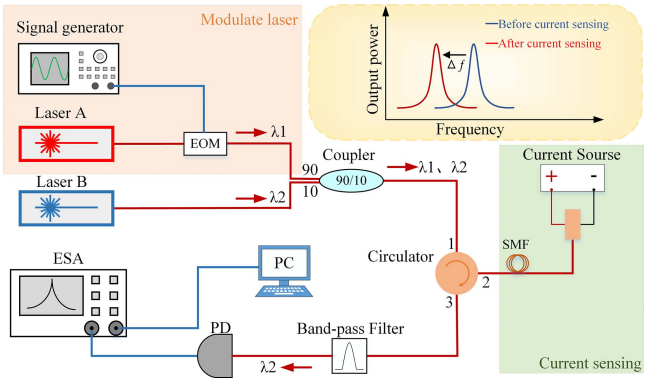

Fig. 4. A diagram of the experimental setup used to generate and receive a signal from the sensor. Legend: EOM = electro optic modulator, PD = photodetector, PC = personal computer, ESA = electric spectrum analyzer.

IV. Current Measurement and Discussion

A diagram of the experimental setup is provided in Fig. 4. Two lasers with different central wavelengths were used to excite the resonator membrane and to detect the induced mechanical vibrations, respectively. Laser A, having a central wavelength of 1549 nm, was used for excitation and was modulated by an electro-optic modulator (Beijing Conquer Optics Science & Technology Co., Ltd.) driven with a sweeping sine signal from 50 to 600 kHz. This laser beam was transmitted to the resonator through a 90:10 coupler and a circulator before reaching the SMF and exciting the vibrational motion of the membrane. The beam was subsequently filtered using a tunable band-pass filter (TBF-1550-1.0-FCAPC, Newport). Exposure to laser A induced periodic fluctuations in the temperature of the graphene/Au membrane that generated thermal forces on the membrane. In response, the membrane would expand and shrink such that the resonator was actuated periodically. A signal was detected using laser B, which was set to emit at a wavelength equivalent to the center of the most intense peak in the reflectance spectrum (1538 nm). This beam was injected into the system through the other port of the coupler and the circulator. The phase difference between the laser beams reflected by the end face of the optical fiber and by the membrane was modulated by the vibration of the membrane, meaning that the intensity of the reflected probe beam was modulated. This reflected beam was received by a photoelectric detector (model 2053, New Fucus, Inc.) and processed using an electrical spectrum analyzer (R&S FSV4, Rohde & Schwarz). Finally, the data from this analyzer were extracted using a computer.

Plots of signal amplitude versus frequency over the range of 100–600 kHz were generated, as shown in Fig. 5(a). Two peaks were observed within this frequency range, corresponding to two thermally excited mechanical resonance modes of the membrane. These appeared at 221.4 and 490.5 kHz and had amplitudes of 5.3 and -2.3 dBm, respectively. These modes were subsequently assessed by generating a simulation model using commercial finite element analysis software and the insets shows the corresponding mode profiles. The mode-shapes are labelled as (m,n), where m refers to the number of nodal diameters and n to the number of nodal circles. Hereafter, the mechanical mode

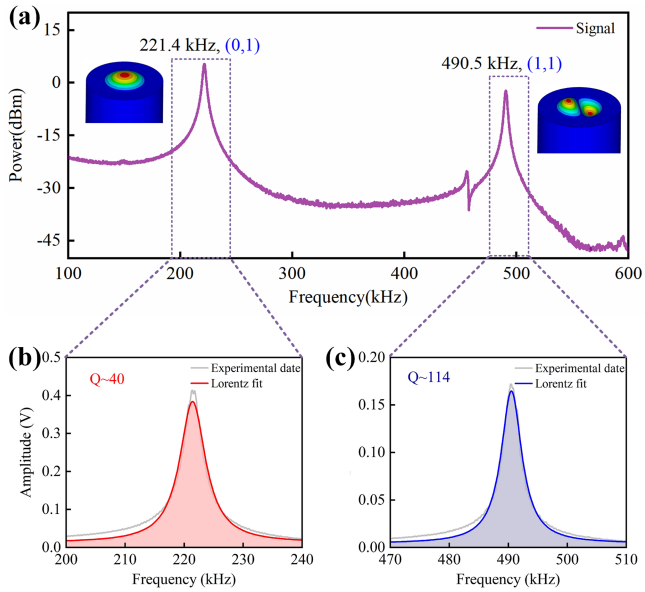

Fig. 5. (a) Mechanical frequency data obtained from the resonator. The insets present images showing the (01) and (11) vibrational modes obtained through finite element simulations. (b-c) Lorentz fitting of the two resonance peaks in linear coordinates.

at 221.4 (first order mode) and 490.5 kHz (second order mode) are referred to as the (0, 1) and (1, 1) mode, respectively. It can be seen that two peaks observed in the (11) mode, which is result of a split degenerate motion typically caused by asymmetric or defective membrane [40]. The amplitude versus frequency curves in linear coordinates fit well to a Lorentzian with the results presented in Fig. 5(b) and (c). Thus we can extract the resonant frequency f_{m}, the full width at half-maximum power (FWHM) Γ, and the quality factor $\mathrm{Q} = f_{\mathrm{m}}/\Gamma$. And the Q values of about 40 and 114 for the frequencies of 221.4 and 490.5 kHz in this resonator, respectively. These Q values are relatively small, possibly as a consequence of energy dissipation in the device, including air damping, thermoelastic damping and surface losses [41], [42].

The two separate electrodes shown in Fig. 1 were used to apply current to the resonator in conjunction with the experimental setup presented in Fig. 4, as a means of evaluating the current response of the resonator. The electric current was generated by an electric current generator (SS-L303SP, Dongguan Bufan Electronics Co., Ltd.). The frequency shifts of the two peaks described above were monitored while increasing the current from 0 to 100 mA in increments of 10 mA. Fig. 6(a) and (b) summarize the variations in the frequency spectra of the resonator as the current was scanned. Both mechanical resonance frequencies are seen to have shifted to lower values as the current was increased as a consequence of changes in the membrane tension [32], [33], [43]. As the current was increased from 0 to 100 mA, the resonant frequencies corresponding to resonance peaks 1 and 2 were found to shift to lower frequencies by 85.5 and 196.9 kHz, respectively.

Fig. 7(a) and (b) summarize the effects of current on the frequencies of resonance peaks 1 and 2, respectively, and indicate that the peak frequency was directly proportional to the square

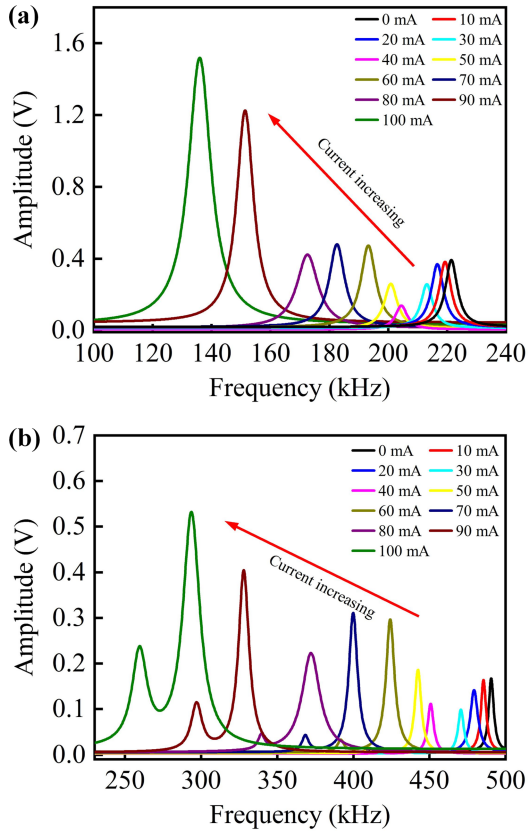

Fig. 6. Evolution of the frequency spectra of the sensor as the current is increased from 0 mA to 100 mA. (a) Resonance peak 1; (b) Resonance peak 2.

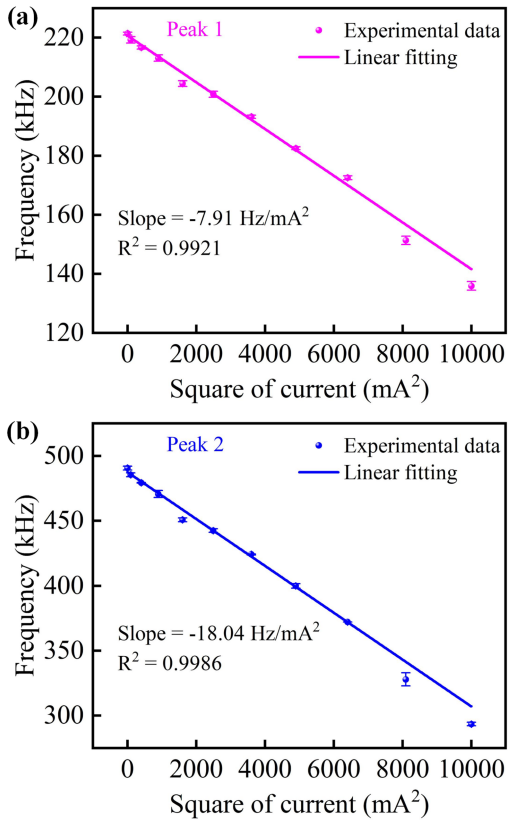

Fig. 7. Resonant frequencies versus current within the range of 0 mA to 100 mA. (a) Resonance peak 1; (b) Resonance peak 2.

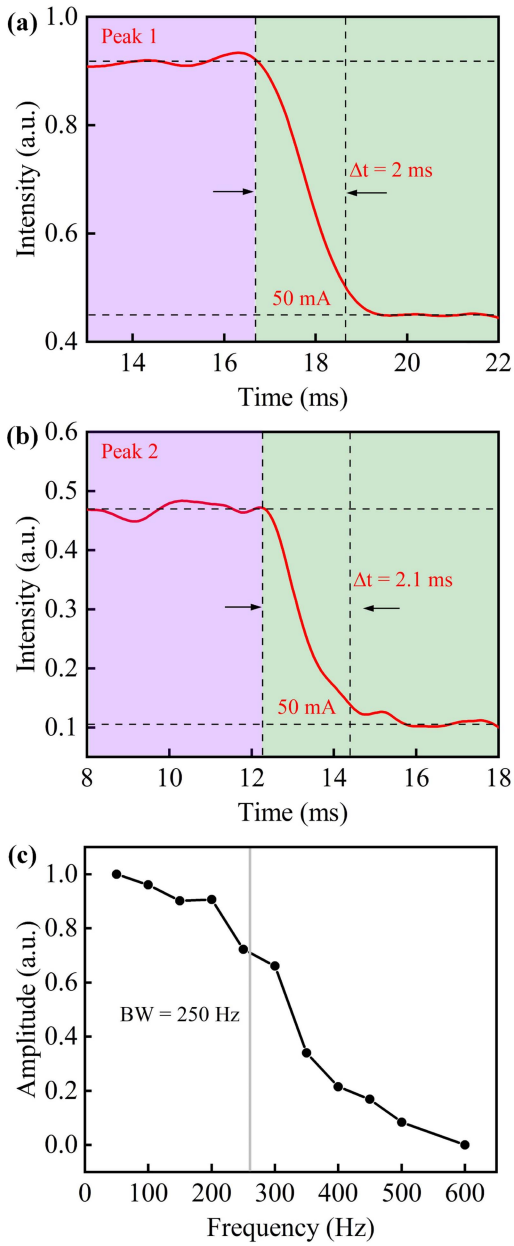

Fig. 8. Time response of resonance peaks 1(a) and 2(b) at 50mA; (c)The frequency bandwidth (BW) of the resonator.

of the current. Three measurements were made at each current value to obtain an error bar, so as to test the stability of the current response of the resonator. The current sensitivity values of the resonator were calculated to be 7.91 and 18.04 Hz/mA^2 for peak 1 and peak 2 based on linear fits. Thus, resonance peak 2 provided higher sensitivity within the same current range, indicating that the sensitivity of this resonator could potentially be improved by monitoring higher order modes.

We studied the time response in both resonant modes by measuring the light intensity change before and after applying current 50 mA. The time responses of both resonant modes are shown in Fig. 8(a) and (b), as the current increasing, the frequency at resonant peak 1 and resonant peak 2 move to a lower frequency, corresponding to light intensity decrease, and

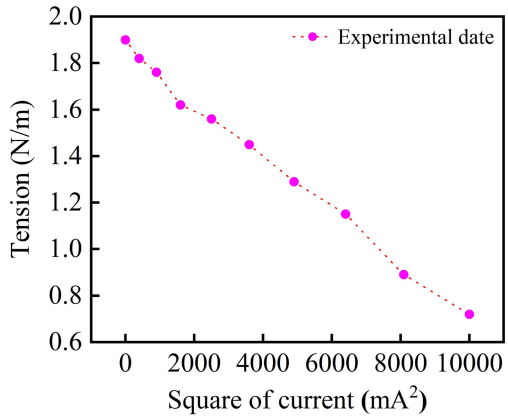

Fig. 9. Estimated membrane tension values as a function of the square of the current.

then reach steady. Where, the sensor response time is defined as the time interval for the sensor to reach 90% of its steady-state response [44], so the time responses applied current 50 mA for both resonance mode are measured to be 2 ms and 2.1 ms, respectively. The frequency bandwidth (BW) is defined as the frequency scope ranging from amplitude maximum to its 3 dB value. To evaluate the frequency bandwidth of the sensor, we plot the amplitude-frequency response curve of the device by applying current at different frequencies, as shown in Fig. 8(c), and the BW of the device response is calculated to be about 250 Hz.

The tension values induced in the membrane by different currents were calculated using Equation (2) based on the resonance frequencies obtained at the various currents. The results summarized in Fig. 9 indicate that the membrane tension was decreased from approximately 1.9 to 0.72 N/m as the current was increased from 0 to 100 mA. Hence, the resonance mode was shifted to lower frequencies as a result of the gradual reduction in thermally induced tension. It is worth noting that these changes in membrane tension resulted from the thermal tension effects of both the graphene and Au. Specifically, the thermal expansion coefficient of graphene is negative while that of Au is positive [45], [46]. Consequently, the thermal tension changes induced by current variations changed in opposite directions for these two membrane materials.

The current response of the resonator was also investigated by monitoring its reflectance spectra, which we refer to as the static measurement method. Fig. 10(a) shows the evolution of the spectrum as the current was increased from 0 to 70 mA. The valley in the spectrum is seen to have shifted toward longer wavelengths as the applied current increased, indicating that the FP cavity was elongated. This effect is attributed to expansion of the membrane induced by the Joule effect. As shown in Fig. 10(b), we study the response of the device to the current through the static measurement method. When the current rises from 0 mA to 100 mA, and the slope of the linear fitting gives a current sensitivity of ~1.18 pm/mA^2 with a correlation factor of R^2 ~0.9848, which shows that the wavelength change has a good linear relationship with the change of the of the current square value. It has previously been proposed that resonators

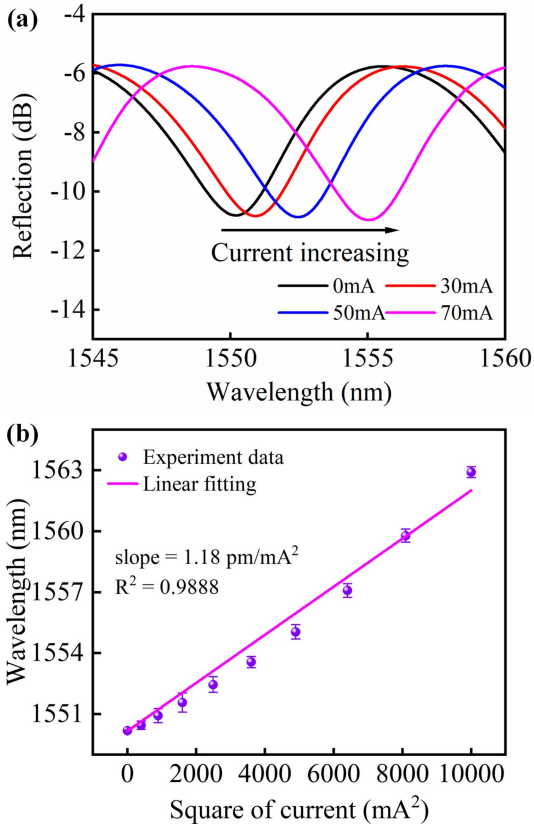

Fig. 10. (a) Reflectance spectra obtained using different currents. (b) Experimentally determined resonance wavelengths as a function of the square of the current.

having thinner Au layers may exhibit higher current sensitivity due to the temperature dependence of conductor's resistance [28]. Thus, a membrane having a thinner Au layer will generate more Joule heat because it has a greater resistance. However, it is preferable to avoid the application of high currents to a resonator with a thinner Au layer because of possible damage to the membrane.

The static measurement range is limited by the FSR, which can be improved by reducing the cavity length, however, the cavity length cannot be infinitely reduced. In addition, the reflectivity of the graphene/Au membrane is much higher than the reflectivity of the optical fiber end face, so the interference fringe contrast will reduce in the process of shorting the cavity length, which brings difficulties to wavelength demodulation. In contrast, there is no such limitation in the optomechanical method, only a certain resonant peak frequency is recorded to demodulate. Moreover, the higher resonant peak frequency is, the higher sensitivity of the device can be achieved.

V. Conclusion

This work demonstrated the first-ever optomechanical cavity current sensor based on a graphene/Au membrane. This device has a large working range of 0-100 mA along with high current sensitivities of approximately 7.91 and 18.04 Hz/mA^2, respectively, for the first and second order vibrational modes at room temperature. The functional element in this sensor is

the graphene/Au membrane, the tension of which changes with variations in temperature resulting from Joule heating when a current is applied. The compact size of this device, the absence of special packaging requirements and the all-fiber construction are expected to allow the proposed sensor to have applications in the sensing of electric and magnetic fields. Furthermore, the proposed nano optomechanical resonator can be used as a basic platform to study the nonlinear dynamics and thermal properties of suspended 2D materials [47], [48], and can also be applied to the specific detection of gas/biomolecules [49], [50] by combining different functional materials.

REFERENCES

[1] S. L. de Bonis et al., "Ultrasensitive displacement noise measurement of carbon nanotube mechanical resonators," *Nano Lett.*, vol. 18, no. 8, pp. 5324–5328, Aug. 2018.

[2] J. Moser et al., "Ultrasensitive force detection with a nanotube mechanical resonator," *Nature Nanotechnol.*, vol. 8, no. 7, pp. 493–496, Jul. 2013.

[3] G. Gruber et al., "Mass sensing for the advanced fabrication of nanomechanical resonators," *Nano Lett.*, vol. 19, no. 10, pp. 6987–6992, Oct. 2019.

[4] C. M. Jiang, Q. K. Li, J. J. Huang, S. Bi, R. N. Ji, and Q. L. Guo, "Single-layer MoS2 mechanical resonant piezo-Sensors with high mass sensitivity," *ACS Appl. Mater. Interfaces*, vol. 12, no. 37, pp. 41991–41998, Sep. 2020.

[5] M. Sansa et al., "Optomechanical mass spectrometry," *Nature Commun.*, vol. 11, no. 1, Jul. 2020, Art. no. 3781.

[6] R. N. Patel, J. P. Mathew, and A. Borah, "Deshmukh. low tension graphene drums for electromechanical pressure sensing," *2D Mater.*, vol. 3, no. 1, Mar. 2016, Art. no. 011003.

[7] A. Blaikie, D. Miller, and B. J. Alemán, "A fast and sensitive room-temperature graphene nanomechanical bolometer," *Nature Commun.*, vol. 10, Oct. 2019, Art. no. 4726.

[8] N. Morell et al., "Optomechanical measurement of thermal transport in two-dimensional mose2 lattices," *Nano Lett.*, vol. 19, no. 5, pp. 3143–3150, Mar. 2019.

[9] M. I. Younis, "Sensing and actuation in MEMS," in *Title of His Published Book*, 1st ed., New York, NY, USA: Springer, 2011, pp. 57–75.

[10] B. B. Li et al., "Ultrabroadband and sensitive cavity optomechanical magnetometry," *Photon. Res.*, vol. 8, no. 7, pp. 1064–1071, Jul. 2020.

[11] S. Forstner et al., "Ultrasensitive optomechanical magnetometry," *Adv. Mater.*, vol. 26, no. 36, pp. 6348–6353, Sep. 2014.

[12] W. Y. Yu, W. C. Jiang, Q. Lin, and T. Lu, "Cavity optomechanical spring sensing of single molecules," *Nature Commun.*, vol. 7, Jul. 2016, Art. no. 12311.

[13] S. Basiri-Esfahani, A. Armin, S. Forstner, and W. P. Bowen, "Precision ultrasound sensing on a chip," *Nature Commun.*, vol. 10, Jan. 2019, Art. no. 132.

[14] M. W. Pruessner, D. Park, T. H. Stievater, D. A. Kozak, and W. S. Rabinovich, "Optomechanical cavities for all-optical photothermal sensing," *ACS Photon.*, vol. 5, no. 8, pp. 3214–3221, Aug. 2018.

[15] T. J. Kippenberg, R. Holzwarth, and S. A. Diddams, "Microresonator-based optical frequency combs," *Science*, vol. 332, no. 6029, pp. 555–559, Apr. 2011.

[16] X. Y. Zhang, Y. H. Zhou, Y. Q. Guo, and X. X. Yi, "Optomechanically induced transparency in optomechanics with both linear and ouadratic coupling," *Phys. Rev. A*, vol. 98, no. 5, Nov. 2018, Art. no. 053802.

[17] D. E. Chang, A. H. Safavi-Naeini, M. Hafezi, and O. Painter, "Slowing and stopping light using an optomechanical crystal array," *New J. Phys.*, vol. 13, Feb, 2011, Art. no. 023003.

[18] M. Bagheri, M. Poot, M. Li, W. P. H. Pernice, and H. X. Tang, "Dynamic manipulation of nanomechanical resonators in the high-amplitude regime and non-volatile mechanical memory operation," *Nature Nanotechnol.*, vol. 6, no. 11, pp. 726–732, Nov. 2011.

[19] N. P. Bullier, A. Pontin, and P. F. Barker, "Quadratic optomechanical cooling of a cavity-levitated nanosphere," *Phys. Rev. Res.*, vol. 3, no. 3, Jul. 2011, Art. no. L032022.

[20] Z. P. Wang, S. Q. Zhang, and L. B. Zhang, "Recent advances in optical current-sensing techniques," *Sens. Actuators, A*, vol. 50, no. 3, pp. 169–175, Sep. 1995.

[21] H. Zhang, Y. S. Qiu, H. Li, A. X. Huang, H. X. Chen, and G. M. Li, "High-current-sensitivity all-fiber current sensor based on fiber loop architecture," *Opt. Exp.*, vol. 20, no. 17, pp. 18591–18599, Aug. 2012.

[22] J. Du, Y. M. Tao, Y. P. Liu, L. Ma, W. J. Zhang, and Z. Y. He, "Highly sensitive and reconfigurable fiber optic current sensor by optical recirculating in a fiber loop," *Opt. Exp.*, vol. 24, no. 16, pp. 17980–17988, Aug. 2016.

[23] M. Belal, Z. Song, Y. Jung, G. Brambilla, and T. P. Newson, "Optical fiber microwire current sensor," *Opt. Lett.*, vol. 35, no. 18, pp. 3045–3047, Sep. 2010.

[24] R. L. Wang, S. Y. Xu, W. Li, and X. H. Wang, "Optical fiber current sensor research: Review and outlook," *Opt. Quantum Electron.*, vol. 48, no. 9, Sep. 2016, Art. no. 442.

[25] A. Dante, J. David, C. C. Carvalho, R. Allil, and M. M. Werneck, "A compact FBG-based magnetostrictive optical current sensor with reduced mass of Terfenol-D," *IEEE Photon. Technol. Lett.*, vol. 31, no. 17, pp. 1461–1464, Sep. 2019.

[26] J. D. Lopez et al., "Fiber-optic current sensor based on FBG and optimized magnetostrictive composite," *IEEE Photon. Technol. Lett.*, vol. 31, no. 24, pp. 1987–1990, Dec. 2019.

[27] J. D. Lopez et al., "Fiber-optic current sensor based on FBG and Terfenol-D with magnetic flux concentration for enhanced sensitivity and linearity," *IEEE Sens. J.*, vol. 20, no. 7, pp. 3572–3578, Apr. 2020.

[28] B. C. Zheng, S. C. Yan, J. H. Chen, G. X. Cui, F. Xu, and Y. Q. Lu, "Miniature optical fiber current sensor based on a graphene membrane," *Laser Photon. Rev.*, vol. 9, no. 5, pp. 517–522, Sep. 2015.

[29] Z. Y. Liu and F. Xu, "Miniature sensor based on fiber-graphene-integrated NEMS," presented at ICOCN, Jul. 2017. [Online]. Available: https://ieeexplore.ieee.org/abstract/document/8121538

[30] R. J. Dolleman, D. Lloyd, J. S. Bunch, H. S. J. van der Zant, and P. G. Steeneken, "Transient thermal characterization of suspended monolayer MoS2," *Phys. Rev. Mater.*, vol. 2, no. 11, Nov. 2018, Art. no. 114008.

[31] F. Ye, J. Lee, and P. X. L. Feng, "Electrothermally tunable graphene resonators operating at very high temperature up to 1200 K," *Nano Lett.*, vol. 18, no. 3, pp. 1678–1685, Mar. 2018.

[32] A. K. Al-Mashaal, G. S. Wood, A. Torin, E. Mastropaolo, M. J. Newton, and R. Cheung, "Tunable graphene-polymer resonators for audio frequency sensing applications," *IEEE Sens. J.*, vol. 19, no. 2, pp. 465–473, Jan. 2019.

[33] A. K. Al-mashaal, G. S. Wood, A. T. orin, E. Mastropaolo, M. J. Newton, and R. Cheung, "Dynamic behavior of ultra large graphene-based membranes using electrothermal transduction," *Appl. Phys. Lett.*, vol. 111, no. 24, Dec. 2017, Art. no. 243503.

[34] C. Lee, X. Wei, J. W. Kysar, and J. Hone, "Measurement of the elastic properties and intrinsic strength of monolayer graphene," *Science*, vol. 321, no. 5887, pp. 385–388, Jul. 2008.

[35] J. Ma, W. Jin, H. F. Xuan, C. Wang, and H. L. Ho, "Fiber-optic ferrule-top nanomechanical resonator with multilayer graphene film," *Opt. Lett.*, vol. 39, no. 16, pp. 4769–4772, Aug. 2014.

[36] N. Sruti and K. Jagannadham, "Electrical conductivity of graphene composites with in and in-ga alloy," *J. Electron. Mater.*, vol. 39, no. 8, pp. 1268–1276, Aug. 2010.

[37] K. L. Chopra, L. C. Bobb, and M. H. Francombe, "Electrical resistivity of thin single-crystal gold films," *J. Appl. Phys.*,vol. 34, no. 6, 1963, Art. no. 1699.

[38] A. C. Crowther, A. Ghassaei, N. Jung, and L. E. Brus, "Strong charge-transfer doping of 1 to 10 layer graphene by nO_2," *ACS Nano*, vol. 6, no. 2, pp. 1865–1875, Feb. 2012.

[39] W. J. Ni et al., "Ultrathin graphene diaphragm-based extrinsic fabry-perot interferometer for ultra-wideband fiber optic acoustic sensing," *Opt. Exp.*, vol. 26, no. 16, pp. 20758–20767, Aug. 2018.

[40] D. Davidovikj, J. J. Slim, S. J. Cartamil-Bueno, H. S. J. van der Zant, P. G. Steeneken, and W. J. Venstra, "Visualizing the motion of graphene nanodrums," *Nano Lett.*, vol. 16, no. 4, pp. 2768–2773, Apr. 2016.

[41] R. A. Barton et al., "High, size-dependent quality factor in an array of graphene mechanical resonators," *Nano. Lett.*, vol. 11, no. 3, pp. 1232–1236, Mar. 2011.

[42] B. Kim et al., "Temperature dependence of quality factor in mems resonators," *J. Microelectromech. Syst.*, vol. 17, no. 3, pp. 755–766, Jun. 2018.

[43] V. Singh et al., "Probing thermal dxpansion of graphene and modal dispersion at low-temperature using graphene nanoelectromechanical systems resonators," *Nanotechnology*, vol. 21, no. 16, Apr. 2010, Art. no. 165204.

[44] J. X. Luo et al., "Fiber optic hydrogen sensor based on a Fabry-Perot interferometer with a fiber Bragg grating and a nanofilm," *Lab Chip*, vol. 21, no. 9, pp. 1752–1758, Mar. 2021.

[45] A. I. Oliva, J. M. Lugo, R. A. Gurubel-Gonzalez, R. J. Centeno, J. E. Corona, and F. Avilés, "Temperature coefficient of resistance and thermal expansion coefficient of 10-nm thick gold films," *Thin Solid Films*, vol. 623, pp. 84–89, Feb. 2017.
[46] Y. D. Yoon, Y. W. Son, and H. Cheong, "Negative thermal expansion coefficient of graphene measured by Raman spectroscopy," *Nano Lett.*, vol. 11, no. 8, pp. 3227–3231, Aug. 2011.
[47] D. Davidovikj, F. Alijani, S. J. Cartamil-Bueno, H. S. J. van der Zant, M. Amabili, and P. G. Steeneken, "Nonlinear dynamic characterization of two-dimensional materials," *Nat. Commun.*, vol. 8, Nov. 2017, Art. no. 1253.
[48] F. Ye, J. Lee, and P. X. L. Feng, "Electrothermally tunable graphene resonators operating at very high temperature up to 1200 K," *Nano Lett.*, vol. 18, no. 3, pp. 1678–1685, Mar. 2018.
[49] A. Y. Zhu, F. Yi, J. C. Reed, H. Zhu, and E. Cubukcu, "Optoelectromechanical multimodal biosensor with graphene active region," *Nano Lett.*, vol. 14, no. 10, pp. 5641–5649, Oct. 2014.
[50] L. Z. Zhang et al., "Octahedral SnO_2/Graphene composites with enhanced gas-sensing performance at room temperature," *ACS Appl. Mater. Interfaces*, vol. 11, no. 13, pp. 12958–12967, Apr. 2019.

Shen Liu was born in Henan, China, in 1986. He received the B.Eng. degree in electronic and information engineering from PLA Air Force No.1Aviation University, Changchun, China, in 2008, the M.S. degree in circuit and system from the Chongqing University of Posts and Telecommunications, Chongqing, China, in 2013, and the Ph.D. degree in optics from Shenzhen University, Shenzhen, China, in 2017. From 2017 to 2018, he was with Aston University, Birmingham, U.K., as a Postdoctoral Fellow. Since September 2018, he has been with Shenzhen University, Shenzhen, China, as an Assistant Professor. He has authored or coauthored 11 patent applications and more than 30 journal and conference papers. His research interests focus on optical fiber sensors, WGMs resonator, and cavity optomechanics.

Peijing Chen was born in Guangdong, China, in 1997. He received the B.E. degree in applied physics and materials from Wuyi University, Jiangmen, Guangdong, in 2020, with a major in optoelectronic engineering. His research interests include the design, fabrication of fiber graphene resonators and their applications.

Junxian Luo was born in Guangxi, China, in 1996. She received the B.S. degree in optoelectronic information science technology and engineering from the Guilin University of Electronic Technology, Guilin, China, in 2018. Her research interests focuses on optical fiber resonator and phase-shifted Bragg grating based on femtosecond laser micro-processing technology.

Yanping Chen was born in Chongqing, China, in 1990. She received the M.S. degree in optical engineering from the Chongqing University of Posts and Telecommunications, Chongqing, China, in 2016. She is currently working toward the Ph.D. degree in optical engineering with Shenzhen University.

Bonan Liu received the master's degree from the University of New South Wales, Sydney, NSW, Australia, in 2019. He is currently working toward the Ph.D. degree with the College of Physics and Optoelectronic Engineering, Shenzhen University, Shenzhen, China. His research interests include fiber-based micro cavity and tilted fiber gratings.

Hang Xiao was born in Fujian, China, in 1998. He received the B.E. degree in electronic science and technology, Minjiang University, Fuzhou, China, in 2020, with a major in optoelectronic engineering. His research interests include the design, fabrication of fiber graphene resonators and their applications.

Wenqi Yan was born in Jiangxi, China, in 1996. She received the B.E. degree in applied physics and materials, from Wuyi University, Jiangmen, Guangdong, in 2018, with a major in optoelectronic engineering. Her research interests include the design, preparation, and research of optical resonators and grating fiber sensing applications.

Wei Ding was born in Anhui, China, in 1998. He received the B.E. degree in mechatronics and automation from Huaqiao University, Quanzhou, China, in 2020 with a major in measurement and control technology and instrument. His research interests include the design, fabrication of fiber graphene resonators and their applications.

Zhiyong Bai received the B.S. degree in physics from Ningbo University, Ningbo, China, in 2008, the M.S. degree in optics from South China Normal University, Guangzhou, China, in 2011, and the Ph.D. degree in optics from Nankai University, Tianjin, China, in 2014. From 2014 to 2015, he has with State Grid Electric Power Research Institute, as a R&D Engineer. Since 2015, he has been a Postdoctoral Research Fellow with the Guangdong and Hong Kong Joint Research Centre for Optical Fiber Sensors, Shenzhen University, Shenzhen, China. He is the author or coauthor of more than 30 journal papers. His research interests include optical fiber gratings, orbital angular momentum, and optical fiber sensors.

Jun He was born in Hubei, China, in 1985. He received the B.Eng. degree in electronic science and technology from Wuhan University, Wuhan, China, in 2006, and the Ph.D. degree in electrical engineering from the Institute of Semiconductors, Chinese Academy of Sciences, Beijing, China, in 2011. From 2011 to 2013, he was with Huawei Technologies, Shenzhen, China, as a Research Engineer. From 2013 to 2015, he was affiliated with Shenzhen University, Shenzhen, China, as a Postdoctoral Research Fellow. From 2015 to 2016, he was with The University of New South Wales, Sydney, NSW, Australia, as a Visiting Fellow. Since 2017, he has been with Shenzhen University, Shenzhen, China, as an Assistant Professor. His research interests include optical fiber sensors, fiber Bragg gratings, and fiber lasers. Dr. He is a Member of the Optical Society of America.

Yiping Wang (Senior Member, IEEE) was born in Chongqing, China, in 1971. He received the B.Eng. degree in precision instrument engineering from the Xi'an Institute of Technology, Xi'an, China, in 1995, and the M.S. and Ph.D. degrees in optical engineering from Chongqing University, Chongqing, China, in 2000 and 2003, respectively. From 2003 to 2005, he was with Shanghai Jiao Tong University, Shanghai, China, as a Postdoctoral Fellow. From 2005 to 2007, he was with the Hong Kong Polytechnic University, Hong Kong, as a Postdoctoral Fellow. From 2007 to 2009, he was with the Institute of Photonic Technology, Jena, Germany, as a Humboldt Research Fellow. From 2009 to 2011, he was with the Optoelectronics Research Centre, University of Southampton, Southampton, U.K., as a Marie Curie Fellow. Since 2012, he has been with Shenzhen University, Shenzhen, China, as a Distinguished Professor. He has authored or coauthored one book, 21 patent applications, and more than 240 journal and conference papers. His research interests include optical fiber sensors, fiber gratings, and photonic crystal fibers. His current research interests include optical fiber sensors, fiber gratings, and photonic crystal fibers. Prof. Wang is a Senior Member of the Optical Society of America, and the Chinese Optical Society.